Proceedings of the
Annual Stability Conference
Structural Stability Research Council
Atlanta, Georgia, April 21-24, 2026

A unified design method for overhanging steel girders

Vahab Esmaeili[1], Ali Imanpour[2], Robert G. Driver[3]

Abstract
This paper introduces a unified design method for predicting the flexural capacity of overhanging steel girders in Gerber roof-framing systems and demonstrates its practical application. The method implicitly accounts for the interaction between cantilever and back-span segments and includes explicit provisions for tension-flange bolt holes. Representative design examples are presented for a five-bay single-story industrial building, considering both single- and double-overhanging girders under five loading and restraint conditions. The design process includes evaluation of flexural and shear capacities, service-level deflection, and web yielding and crippling at load-application points, including column lines. The results confirm the practicality of the method for routine design while highlighting over-conservatism associated with a specific loading and restraint condition and the need for improved guidance on bottom-flange bracing requirements at column lines.

1. Introduction

Overhanging steel girders are key structural components in cantilever–suspended-span construction—commonly referred to as the Gerber system in Canada and as beam-over-column framing in the United States—and are widely used in the roof framing of large single-story buildings. As shown in Fig. 1, by extending alternate-bay girders beyond their supports to carry intermediate drop-in segments, the system permits negative moments to develop at column lines, producing a more balanced bending-moment distribution than that of simply-supported arrangements. This configuration can result in reduced girder depth and weight, improved deflection performance, and efficient fabrication and erection. Despite these advantages, the structural behavior of overhanging girders is complex and potentially vulnerable to instability—particularly lateral–torsional buckling (LTB). This complexity arises from the interaction between the cantilever and back-span segments, the presence of reverse-curvature bending, and the wide range of possible loading and restraint conditions (LRCs) encountered in practice. A critical requirement for stability is the provision of effective restraint against both lateral displacement and cross-sectional twisting at column lines; however, such restraint is often difficult to achieve in practice—especially for the bottom flange, which typically lacks the support provided to the top

[1] Postdoctoral Fellow, University of Alberta, <vahab@ualberta.ca>
[2] Associate Professor, University of Alberta, <imanpour@ualberta.ca>
[3] Professor Emeritus, University of Alberta, <rdriver@ualberta.ca>

flange by the roof deck. Additional complications arise from practical detailing requirements, such as bolt holes in the top flange at joist-to-girder connections, which may compromise flexural ductility in negative-moment regions if not properly accounted for.

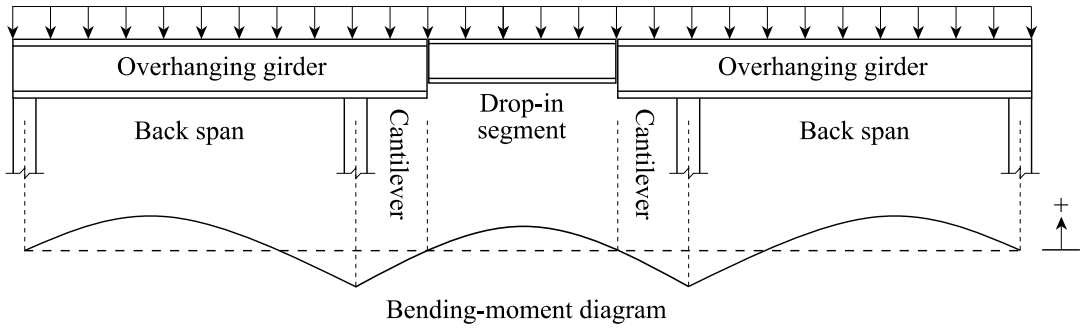

Figure 1: Schematic of a Gerber roof-framing system and its bending-moment distribution (Esmaeili 2025).

Current North American steel design standards—including the CSA Design and Construction of Steel Structures, CSA S16 (CSA 2024), and the AISC Specification for Structural Steel Buildings, AISC 360 (AISC 2022)—do not provide unified provisions specifically tailored to overhanging girders, leaving designers to rely on disparate recommendations available in the technical literature. Existing methods have generally been developed for narrowly-defined conditions, and their effectiveness varies with loading, support, and bracing configurations; when applied beyond their intended scope, they may become overly conservative or unconservative, potentially leading to inefficient or unsafe designs (Esmaeili et al. 2025). To address these limitations and avoid fragmented design procedures, a unified design method was recently developed (Esmaeili 2025). The objective of the present paper is to briefly introduce this method and demonstrate its application through practical design examples of Gerber roof-framing systems. The examples consider interior roof framing of a five-bay single-story industrial building and include both single- and double-overhanging girders under various LRCs. Emphasis is placed on illustrating routine implementation of the method, identifying governing limit states, and highlighting the influence of load patterns, restraint conditions, and tension-flange bolt holes on girder selection.

2. Background Studies

Early work by Nethercot (1973) introduced a design approach for overhanging girders based on the notional effective-length concept. In this formulation, the cantilever segment is idealized as a girder restrained against lateral displacement and twisting at both ends and subjected to uniform bending, with its elastic LTB moment resistance under the actual boundary conditions represented by that of the idealized girder through an effective length. In applying this concept, the cantilever tip—when restrained—is assumed to be restrained at the shear-center level, while the back span—taken to be equal in length to the cantilever—is assumed to be free of loads and restraints between supports. This representation does not explicitly capture the influence of the back-span bay dimension on the stability of the overall system. To address this limitation, Kirby and Nethercot (1979) proposed limiting the cantilever effective length to a minimum equal to the back-span length. Subsequent investigations have shown that this assumption can be overly conservative, particularly when the back span is significantly longer than the cantilever and lateral restraints are present between supports (Esmaeili et al. 2025). A different set of effective-length factors for overhanging girders was later proposed by the Canadian Institute of Steel Construction (CISC 1989).

Essa and Kennedy (1994) developed an interaction method for estimating the elastic LTB moment resistance of overhanging girders in cases where the cantilever segment is more critical than the back span, assuming that the two segments act independently. The method assumes that the back span is free of restraints between the two supports. Elastic LTB moment resistances are first calculated separately for the cantilever and back-span segments, assuming free-to-warp conditions at the supports. Based on finite-element analysis (FEA) results from various rolled wide-flange sections, predictive equations were proposed for cantilevers subjected to two loading conditions: (1) loading at the top-flange level; and (2) loading at the shear-center level. To obtain the elastic LTB moment resistance of the overall system, interaction equations were formulated for two cantilever-tip restraint conditions: (1) an unrestrained tip; and (2) a tip restrained laterally at the top-flange level only. When both the top and bottom flanges are laterally restrained at the cantilever tip, Essa and Kennedy (1994) recommended using the interaction procedures presented in the SSRC Guide (Galambos 1988) or those proposed by Schmitke and Kennedy (1985). For cases in which the back span is more critical than the cantilever, the elastic LTB moment resistance was recommended to be taken as that of the back span alone (Trahair 1983). Subsequent numerical investigations have shown that the approach proposed by Essa and Kennedy (1994) can be overly conservative when the elastic LTB moment resistance of the back span is evaluated without accounting for the beneficial effects of top-flange bracing between supports, particularly when the response is governed by negative moments near the supports (Esmaeili et al. 2025). Essa and Kennedy (1995) also presented a set of 12 design curves for overhanging girders, accounting for the effects of both lateral and torsional restraints.

Yura and Helwig (2010) investigated the stability behavior of girders restrained against lateral displacement and twisting at both ends and subjected to reverse-curvature bending, a condition representative of the back span of overhanging girders if warping restraint at the supports is neglected. Using FEA, they proposed LTB modification factors for two idealized restraint scenarios: (1) girders without restraints between supports; and (2) girders with continuous restraint of the top flange, provided either laterally or torsionally, but not both simultaneously. An additional equation was developed to estimate the elastic LTB moment resistance of composite girders in which the top flange is continuously restrained against both lateral displacement and torsional rotation. Their results indicated that torsional restraint generally has a greater stabilizing influence than lateral restraint, except for girders exhibiting two points of contraflexure when the ratio of the centerline moment to the maximum negative support moment is less than −1.0. The study further showed that the proposed LTB modification factor for girders with continuous lateral bracing of the top flange may be unconservative for reverse-curvature bending in girders exhibiting two points of contraflexure, particularly for members with a length-to-depth ratio of approximately 15 and when the ratio of the moment at the girder centerline to the maximum negative support moment ranges from −0.75 to 1.0. These limitations, however, are not explicitly identified in the AISC 360-22 Commentary, where the modification factor is introduced for gravity-loaded rolled I-section girders with laterally-restrained top flanges.

The CISC Design Module 3 (CISC 2019) provides tabulated design guidance for Gerber roof-framing systems. The tables were developed using FEA and are intended to facilitate section selection for buildings with flat roofs, uniform bay dimensions and cantilever lengths, and evenly-spaced columns and joists, accounting for dead, live, snow, and vertical wind loads representative of Canadian climatic conditions. Equal joist reactions are assumed in each bay, with both joist

loads and drop-in segment reactions applied at the top-flange level of the girders. The top flange is assumed to be laterally restrained at joist locations along the back span and along any cantilevers with lengths exceeding the joist spacing. Three bottom-flange bracing configurations are considered: (1) restraint at column lines only; (2) restraint at column lines and near cantilever tips when the cantilever exceeds the joist spacing; and (3) restraint at column lines and at the back-span joists nearest the interior columns when the cantilever is shorter than the joist spacing.

A research program involving physical testing and numerical modeling has been carried out at the University of Alberta to investigate the stability behavior and design of overhanging girders (Essa 2024; Essa et al. 2024; Imanpour 2024; Datoo 2025; Esmaeili 2025; Esmaeili et al. 2025). Essa (2024) conducted tests on 13 single-overhanging girders fabricated from W410×85 sections, while Datoo (2025) tested 9 double-overhanging W460×97 girders. All specimens had a back-span length of 9.15 m and were subjected to discrete point loads representative of joist reactions, with four equally spaced loads applied along the back span at 1.83-m intervals. Cantilever loads were applied at a distance of 1.83 m from the column line for both single- and double-overhanging configurations. The experimental program investigated several lateral restraint conditions at the cantilever tip, including: (1) unrestrained tips; (2) restraint at the top-flange level only; and (3) combined restraint at both the top and bottom flanges. In addition, the influence of an auxiliary bottom-flange lateral brace at the back-span load point nearest to the column line was examined. In all tests, the top flange was laterally restrained at back-span load points. The experimental results were used to validate a finite-element model developed by Esmaeili (2025) that captures material and geometric nonlinearities, residual stresses, initial imperfections, and cross-sectional distortion. The validated model was subsequently employed to generate a large dataset covering a wide range of loading, restraint, and geometric configurations relevant to overhanging girders. This dataset enabled evaluation of existing design approaches and identification of key parameters governing LTB moment resistance (Esmaeili et al. 2025). Based on these findings, Esmaeili (2025) proposed a unified design equation to predict the moment resistance of overhanging girders over a broad range of LRCs. The proposed equation implicitly accounts for cantilever–back-span interaction and provides the ultimate moment resistance directly, without requiring prior elastic LTB calculations. The numerical framework was further extended to investigate the influence of bolt holes in the tension flange at joist-to-girder connections in negative-moment regions, leading to design recommendations intended to achieve the predicted moment resistance while preserving flexural ductility in the presence of flange holes. The present paper first introduces this design method and then demonstrates its application through representative design examples for Gerber roof-framing systems.

3. Overview of Design Method for Overhanging Girders

This section summarizes the design method proposed by Esmaeili (2025) and used in this paper to: (1) calculate the moment resistance of overhanging girders, accounting for LTB and plastic hinge formation; and (2) address the effect of bolt holes in the tension flange at column lines.

3.1 Range of Applicability

Fig. 2 illustrates the configuration of a typical overhanging girder, its bending-moment diagram, and the relevant geometric and loading parameters.

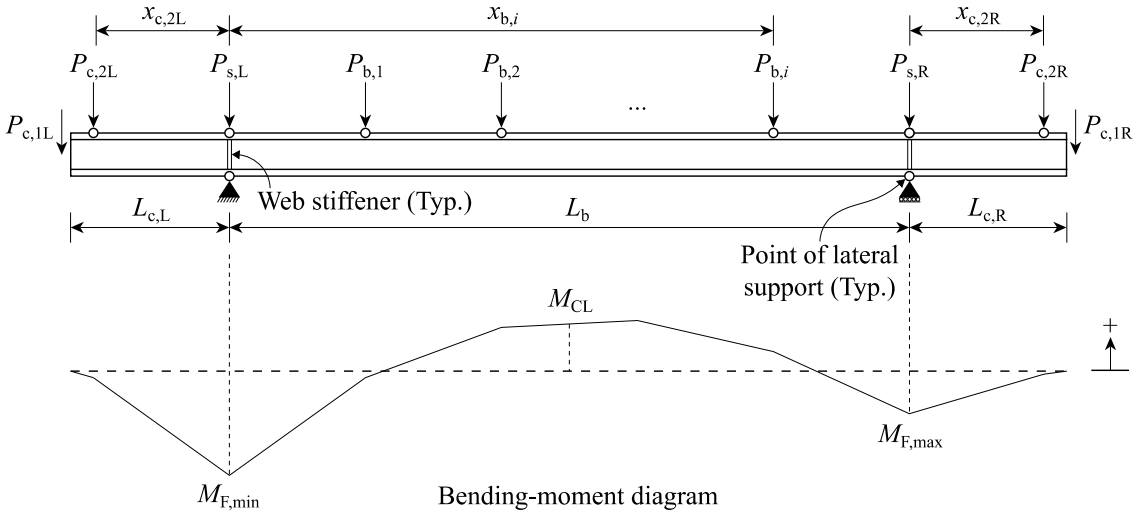

Figure 2: Configuration of a typical overhanging girder and its corresponding bending-moment diagram.

The girder in Fig. 2 consists of a back span of length L_b and one or two cantilever segments of lengths $L_{c,L}$ and $L_{c,R}$ at the left and right ends, respectively. A single-overhanging girder is treated as a special case in which one cantilever length is zero. The back span is subjected to a series of point loads $P_{b,i}$, representing reactions from joists framing into the girder. These loads are applied at locations $x_{b,i}$, measured from the left support, and are typically introduced at the top-flange level, where the joists also provide lateral restraint to the top flange. Joist reactions at the left and right supports are denoted by $P_{s,L}$ and $P_{s,R}$, respectively. Each cantilever may carry one or two point loads. The loads $P_{c,1L}$ and $P_{c,1R}$ denote the concentrated loads applied at the left and right cantilever tips, respectively, and represent the reaction from the drop-in segment supported by the corresponding cantilever. These loads are commonly applied at, or slightly above, the shear-center level. In addition, loads $P_{c,2L}$ and $P_{c,2R}$ may be present when joists frame directly into the cantilevers; these loads act at distances $x_{c,2L}$ and $x_{c,2R}$ from the left and right supports, respectively, and are applied at the top-flange level. Note that all applied loads may act downward or upward. The bending-moment diagram is characterized by the moment at the centerline of the back span, M_{CL}, and by the moments at the support locations. The algebraically smaller and larger support moments are denoted by $M_{F,min}$ and $M_{F,max}$, respectively; all moment quantities retain the signs indicated in Fig. 2.

The design method applies to overhanging girders with wide-flange sections that satisfy the width-to-thickness ratio limits for Class 1 (seismically compact) or Class 2 (compact) sections specified in CSA S16-24. These limits are expressed as $b/(2t) \leq 170/(F_y)^{0.5}$ and $h/w \leq 1700/(F_y)^{0.5}$—where b denotes the flange width; t is the flange thickness; h signifies the clear depth of the web; w is the web thickness; and F_y is the minimum specified yield strength of steel. In addition, lateral displacement, cross-sectional twisting, and distortion must be restrained at support locations. In particular, distortion at support locations is prevented by providing appropriate web stiffeners, as illustrated in Fig. 2, even when the factored bearing resistance of the web—in accordance with CSA S16-24—is not exceeded. The minimum required stiffener thickness is such that the width-to-thickness ratio of each stiffener plate does not exceed the local buckling limit of $200/(F_{ys})^{0.5}$, where F_{ys} is the minimum specified yield strength of the stiffener material.

The proposed design method provides solutions for five LRCs, illustrated in Fig. 3, as follows: (1) the cantilever tip is loaded at the shear-center level and unrestrained (LRC 1); (2) the cantilever tip is loaded at the top-flange level for downward loads and at the shear-center level for upward loads, while being laterally restrained at the top-flange level regardless of the load direction (LRC 2); (3) the cantilever tip is loaded at the top-flange level and laterally restrained at both the top and bottom flanges (LRC 3); (4) similar to LRC 1, but with additional bottom-flange lateral restraints in the back span positioned at the load points nearest to the interior supports (LRC 4); and (5) similar to LRC 3, but with additional bottom-flange lateral restraints in the back span positioned at the load points nearest to the interior supports (LRC 5).

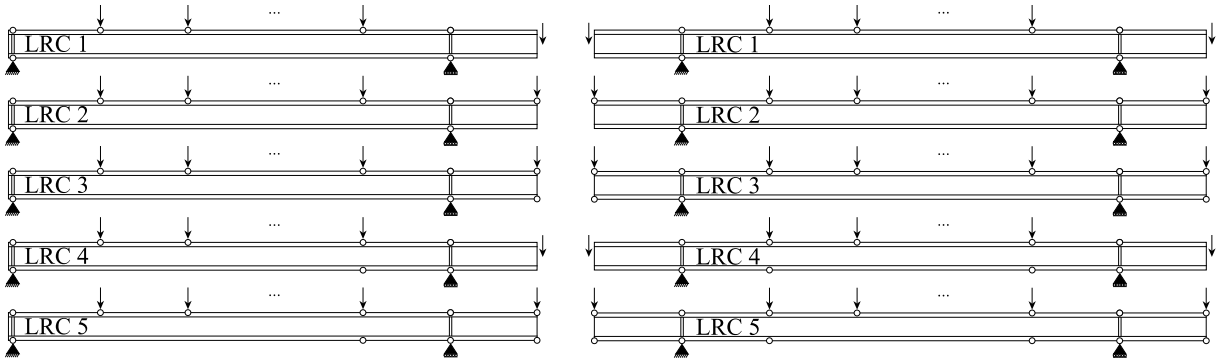

(a) (b)

Figure 3: LRCs: (a) single-overhanging girder; and (b) double-overhanging girder.

3.2 Moment Resistance

Following limit-states design methodology, for overhanging girders that fall within the range of applicability defined in Section 3.1, the factored moment resistance, M_r, is expressed as:

$$M_r = \phi \Omega_2 M_p \leq \phi M_p \tag{1}$$

where ϕ is the resistance factor, taken as 0.9; M_p is the plastic moment capacity of the cross-section about the strong axis; and Ω_2 is calculated as:

$$\Omega_2 = \xi \left(\frac{M'_{u,b}}{M_p} \right)^{\psi_0} \left(1 - \frac{\kappa'_1}{2} \right)^{\psi_1} \left(1 - \frac{\kappa'_2}{2} \right)^{\psi_2} \left(1 - \frac{\kappa'_3}{2} \right)^{\psi_3} \left(\frac{h}{w} \right)^{\psi_4} \left(3 - n_c \right)^{\psi_5} \tag{2}$$

in which $M'_{u,b}$ is computed as:

$$M'_{u,b} = \frac{\pi}{L_b} \sqrt{EI_y GJ + \left(\frac{\pi E}{L_b} \right)^2 I_y C_w} \tag{3}$$

where E and G are the elastic and shear moduli of steel, respectively; I_y represents the moment of inertia about the weak axis of the cross-section; and J and C_w denote the St. Venant and warping torsional constants, respectively. The moment ratios κ'_1, κ'_2, and κ'_3 characterize the shape of the bending-moment diagram and are defined as M_{CL}/M_{max}, $M_{F,min}/M_{max}$, and $M_{F,max}/M_{max}$, respectively—where M_{max} is the maximum moment magnitude along the girder, including sign.

The variable n_c is the number of cantilever segments, with $n_c = 1$ for a single-overhanging girder and $n_c = 2$ for a double-overhanging girder. The coefficient ξ and the exponents ψ_0 through ψ_5 are selected from Table 1 based on the signs of M_{max} and κ'_1, as well as the LRC of the girder.

Table 1: Coefficients and exponents for calculating Ω_2

Maximum-moment orientation	Moment distribution	LRC	ξ	ψ_0	ψ_1	ψ_2	ψ_3	ψ_4	ψ_5
$M_{max} > 0$	$\kappa'_1 \geq 0$	1	2.09	0.34	−0.55	−1.66	−0.68	0	0
		2	22.71	0.33	−0.64	−3.13	−0.61	−0.60	−0.04
		3	0.97	0	0	0	0	0	0
		4	0.97	0	0	0	0	0	0
		5	0.98	0	0	0	0	0	0
	$\kappa'_1 < 0$	1	6.89	0.58	−4.61	−0.42	0	0	−0.14
		2	6.53	0.57	−4.47	−0.36	0	0	−0.15
		3	6.93	0.56	−4.16	−0.22	0	0	−0.32
		4	7.38	0.53	−4.04	−0.16	0	0	−0.48
		5	8.24	0.54	−4.28	−0.16	0	0	−0.51
$M_{max} < 0$	$\kappa'_1 \geq 0$	1	11.06	0.58	1.13	0.50	0.22	−0.43	−0.04
		2	12.11	0.53	0.88	0.59	0.27	−0.51	−0.03
		3	2.87	0.64	1.08	0.35	0	0	−0.17
		4	3.41	0.55	1.20	0.19	0	0	−0.32
		5	3.63	0.54	1.29	0.20	0	0	−0.33
	$\kappa'_1 < 0$	1	14.67	0.51	0.59	0	0.45	−0.56	−0.04
		2	18.00	0.33	0.28	0	0.27	−0.79	−0.04
		3	1.81	0.39	0.33	0	0.28	0	−0.10
		4	0.98	0	0	0	0	0	0
		5	0.98	0	0	0	0	0	0

3.3 Effect of Tension-Flange Bolt Holes

At joist-to-girder connections, bolt holes are commonly required in the top flange of overhanging girders—whether introduced for temporary field erection or as part of permanent bolted joist connections. When located in negative-moment regions, typically at support locations, the top flange is in tension, and such holes introduce localized tensile stress concentrations that increase the risk of net-section fracture and may reduce the girder's flexural ductility. The design method therefore includes specific recommendations for accounting for the effect of tension-flange bolt holes on the moment resistance of overhanging girders. Accordingly, assuming the cross-section meets the requirements for Class 1 or Class 2 sections in accordance with CSA S16-24 and that $F_y \leq 350$ MPa, the use of gross cross-sectional properties in calculating the moment resistance of an overhanging girder is permitted when either: (1) the tension-flange bolt holes occupy no more than 15% of the gross flange area; or (2) the tension-flange bolt holes occupy no more than 25% of the gross flange area and the flange is classified as Class 1. If neither condition is satisfied—regardless of the location of maximum moment magnitude—M_p must be reduced using the effective plastic section modulus, Z_e, calculated as (CSA 2024):

$$Z_e = \min(0.05Z + Z_n , Z) \tag{4}$$

where Z and Z_n are the plastic section moduli of the gross and net cross-sections, respectively. Assuming two bolt holes are present in the tension flange at a single girder cross-section, Z_n is calculated as:

$$Z_n = Z - \rho_h A_{fg}\left(\frac{d-t}{2} + \frac{A_{fg} - A_{fn}}{2w}\right) + w\left(\frac{A_{fg} - A_{fn}}{2w}\right)^2 \tag{5}$$

in which ρ_h represents the fractional reduction in the tension-flange area; A_{fg} denotes the gross area of the tension flange; d is the overall depth of the cross-section; A_{fn} is the net area of the tension flange; and the remaining variables have been defined previously.

4. Design Examples

Ten design examples (comprising single- and double-overhanging girders each evaluated under five LRCs) are presented to demonstrate the application of the design method described in Section 3 to practical roof-framing systems.

4.1 Building Description: Geometric, Loading, and Restraint Conditions

The design examples consider the interior five-bay roof framing of a single-story industrial building. The framing system consists of a central double-overhanging girder, two single-overhanging girders at the ends of the building, and drop-in segments spanning between adjacent cantilever tips, as illustrated in Fig. 4. The girders support joists on both sides—at column lines and at evenly-spaced locations within each bay. The joists frame into the girders at a spacing of s = 1.71 m and are connected using bolted connections. At these locations, the joists are assumed to provide lateral restraint to the top flange of the girder. Any torsional restraint that may be afforded by the joists is conservatively neglected. At column lines, the bottom flange is laterally restrained through bottom-chord extensions of the joists, and web stiffeners are provided to prevent cross-sectional distortion. Table 2 summarizes the geometric parameters used in the design examples.

Table 2: Summary of building geometric parameters for the design examples

Geometric parameter	Symbol	Value
Column spacing or back-span length	L_b	12.0 m
Cantilever length	L_c	1.5 m (LRCs 1 and 4) and 2.0 m (LRCs 2, 3, and 5)
Joist span	L_j	10.0 m
Number of joist spaces in each bay	n	7
Joist spacing	s	1.71 m
Length of drop-in segments	L_d	9.0 m (LRCs 1 and 4) and 8.0 m (LRCs 2, 3, and 5)
Building height	H	15.0 m
Smaller plan dimension of roof	L_1	60.0 m (parallel to the frame)
Larger plan dimension of roof	L_2	70.0 m (perpendicular to the frame)

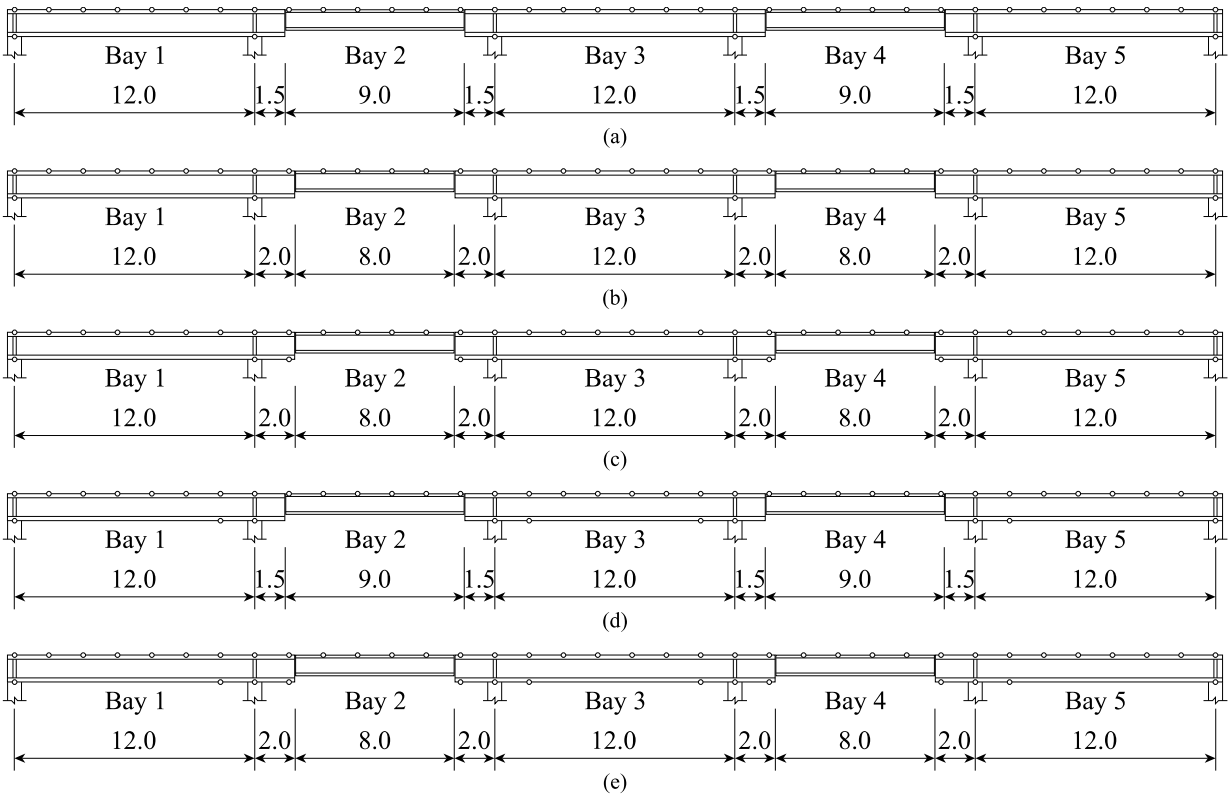

Figure 4: Roof-framing configurations used in the design examples (dimensions in m), corresponding to: (a) LRC 1; (b) LRC 2; (c) LRC 3; (d) LRC 4; and (e) LRC 5.

Five roof-framing configurations are considered in the design examples, corresponding to the five LRCs introduced in Section 3. These configurations are illustrated in Fig. 4 and differ primarily in cantilever length and the use of bottom-flange lateral restraints. In Configuration 1 (Fig. 4a), the cantilever length is shorter than the joist spacing and therefore remains unrestrained along its length, with bottom-flange lateral restraint provided only at column lines. The overhanging girders in this configuration are evaluated using LRC 1. In Configuration 2 (Fig. 4b), the cantilever length exceeds the joist spacing and is consequently laterally restrained at the top-flange level near the cantilever tip, while bottom-flange lateral restraint is again provided only at column lines. For design, the cantilever load is conservatively assumed to act entirely at the top-flange level for downward loading and at the shear-center level for upward loading; under this assumption, the overhanging girders are evaluated using LRC 2. Configuration 3 (Fig. 4c) is identical to Configuration 2, except that an additional bottom-flange lateral restraint is provided near the cantilever tip. Accordingly, the overhanging girders are evaluated using LRC 3. In Configuration 4 (Fig. 4d), the framing is similar to Configuration 1 but includes additional bottom-flange lateral restraints in the back span, located at a distance equal to the joist spacing from the interior support. One such restraint is provided for single-overhanging girders and two (one adjacent to each interior support) for the double-overhanging girder. This configuration corresponds to LRC 4. Finally, Configuration 5 (Fig. 4e) is similar to Configuration 3, but includes additional bottom-flange lateral restraints in the back span at a distance equal to the joist spacing from the interior support. The overhanging girders in this configuration are therefore evaluated using LRC 5.

4.2 Design Loads

Loads are determined in accordance with the National Building Code (NBC) of Canada (NRC 2020), assuming a building of normal importance located on open, flat terrain in Edmonton, Alberta, with large openings and a flat roof without significant rooftop features. The building is situated neither in a rural area nor in an exposed location north of the treeline. Lateral loads due to wind and earthquake effects are not considered, as the framing system examined does not include elements that form part of the lateral load path (e.g., diaphragm chords or collectors). A dead load of 1.50 kPa is assumed, inclusive of the self-weight of the girders and joists. The roof live load is taken as 1.00 kPa, with no reduction permitted for tributary area. Snow and vertical wind loads are determined in accordance with NBC provisions; detailed derivations are reported by Esmaeili (2025).

Pattern loading is of particular importance for roof-framing systems incorporating overhanging girders, as it can produce the most severe load effects. Representative load patterns used in the design examples are illustrated in Figs. 5 and 6. Although shown as line loads for clarity, these represent area loads distributed over tributary widths perpendicular to the plane of the frame. In the notation used herein, *DL*, *LL*, *SL*, *DWL*, and *UWL* refer to dead, live, snow, downward wind, and upward wind load types, respectively—regardless of pattern. A subscript "0" denotes a full-pattern load case (e.g., LL_0 in Fig. 5b), while non-zero subscripts indicate partial-pattern cases (e.g., LL_1 and LL_2 in Fig. 5b). In Fig. 5, $D_F = 1.50$ kPa represents the intensity of the full dead load; $L_F = 1.00$ kPa is the intensity of the full live load; and $S_F = 1.46$ kPa is the intensity of the full snow load. In Fig. 6, $W_{D,F} = 0.77$ kPa denotes the full downward wind pressure, while $W_{U,F} = -1.33$ kPa and $1.18W_{U,F} = -1.57$ kPa represent the full upward wind pressures (including both internal and external pressure effects) applied in the interior and end zones, respectively. A reduced upward wind pressure of $0.45W_{U,F} = -0.59$ kPa is also considered, corresponding to cases in which external pressure is absent and only internal pressure is present. Dead load and downward wind load are applied only as full-pattern loads, as shown in Figs. 5a and 6a, respectively.

4.3 Load Combinations

Load combinations for the ultimate limit states (ULS) and serviceability limit states (SLS) are summarized in Table 3. For ULS combinations, live and snow loads are not applied simultaneously, in accordance with the NBC. For SLS combinations, dead load is excluded on the assumption that it is sustained throughout the life of the building and can potentially be offset through camber.

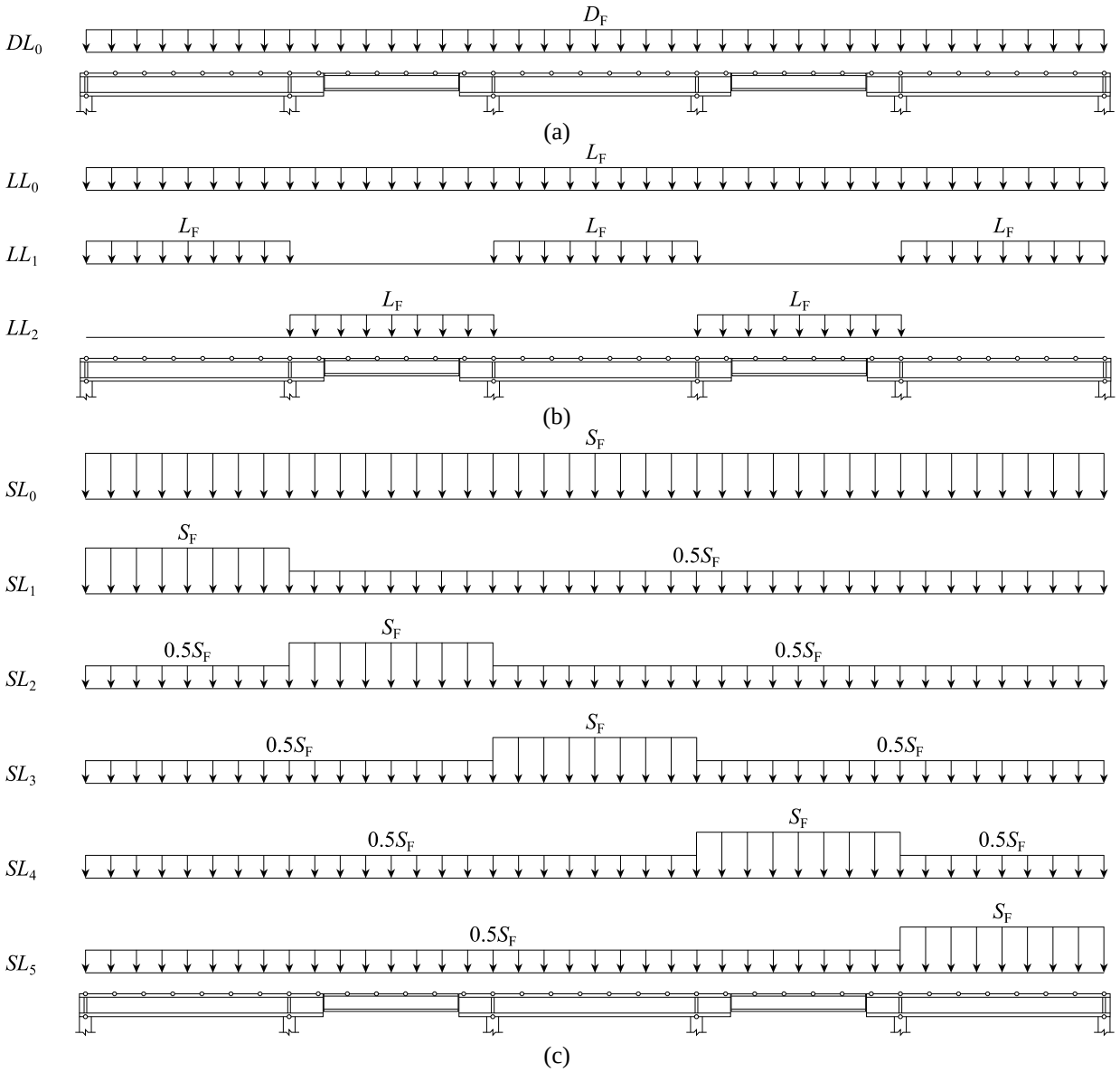

Figure 5: Load patterns for gravity loads: (a) dead load (*DL*); (b) live load (*LL*); and (c) snow load (*SL*).

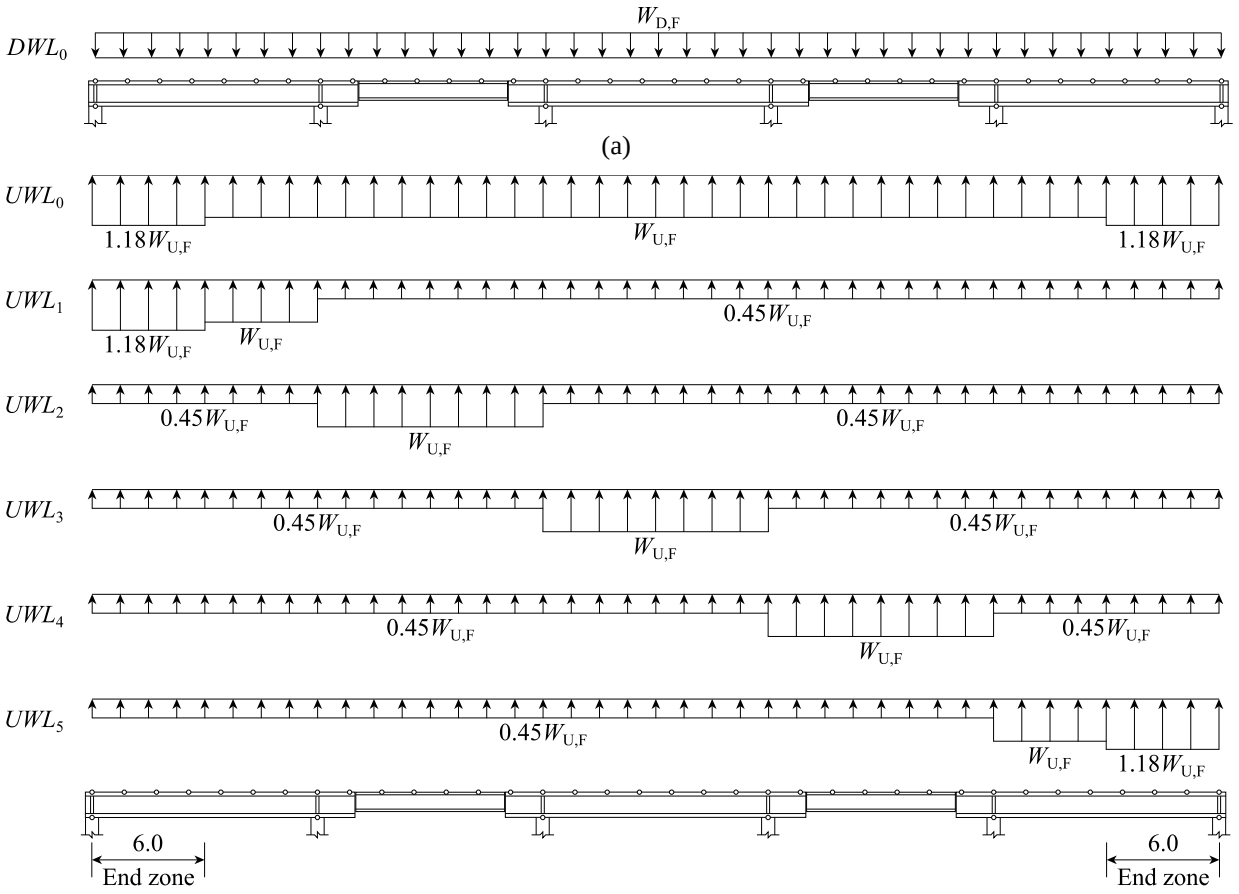

Figure 6: Load patterns for vertical wind load (dimensions in m):
(a) downward wind load (*DWL*); and (b) upward wind load (*UWL*).

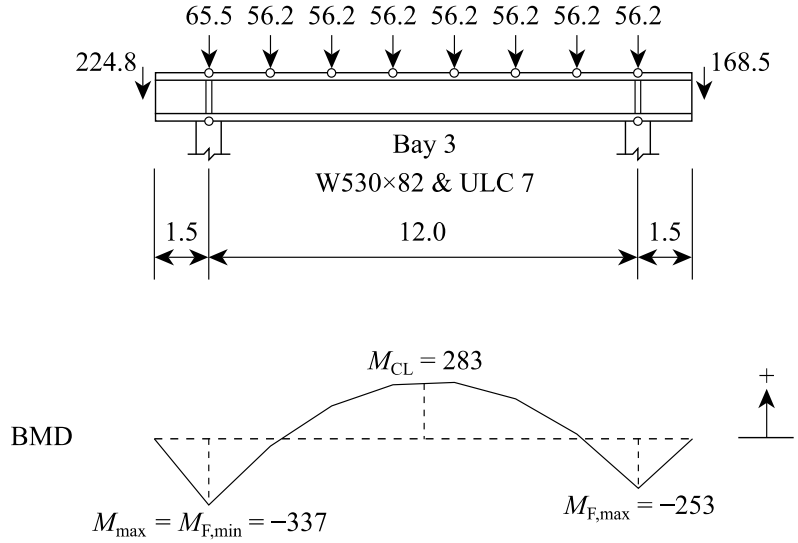

Figure 7: BMDs for the W530×82 double-overhanging girder under LRC 1 and ULC 7
(dimensions in m, loads in kN, and moments in kN·m).

Table 3: Load combinations

ULS		SLS[a]	
ID	Description	ID	Description
ULC 1	$1.4DL_0$	SLC 1	$1.0LL_0 + 0.3(0.75DWL_0)$
ULC 2	$1.25DL_0 + 1.5LL_0 + 0.4DWL_0$	SLC 2	$1.0LL_1 + 0.3(0.75DWL_0)$
ULC 3	$1.25DL_0 + 1.5LL_1 + 0.4DWL_0$	SLC 3	$1.0LL_2 + 0.3(0.75DWL_0)$
ULC 4	$1.25DL_0 + 1.5LL_2 + 0.4DWL_0$	SLC 4	$1.0(0.9SL_0) + 0.3(0.75DWL_0)$
ULC 5	$1.25DL_0 + 1.5SL_0 + 0.4DWL_0$	SLC 5	$1.0(0.9SL_1) + 0.3(0.75DWL_0)$
ULC 6	$1.25DL_0 + 1.5SL_1 + 0.4DWL_0$	SLC 6	$1.0(0.9SL_2) + 0.3(0.75DWL_0)$
ULC 7	$1.25DL_0 + 1.5SL_2 + 0.4DWL_0$	SLC 7	$1.0(0.9SL_3) + 0.3(0.75DWL_0)$
ULC 8	$1.25DL_0 + 1.5SL_3 + 0.4DWL_0$	SLC 8	$1.0(0.9SL_4) + 0.3(0.75DWL_0)$
ULC 9	$1.25DL_0 + 1.5SL_4 + 0.4DWL_0$	SLC 9	$1.0(0.9SL_5) + 0.3(0.75DWL_0)$
ULC 10	$1.25DL_0 + 1.5SL_5 + 0.4DWL_0$	SLC 10	$1.0(0.75DWL_0) + 0.35(0.9SL_0)$
ULC 11	$1.25DL_0 + 1.4DWL_0 + 0.5SL_0$	SLC 11	$1.0(0.75DWL_0) + 0.35(0.9SL_1)$
ULC 12	$1.25DL_0 + 1.4DWL_0 + 0.5SL_1$	SLC 12	$1.0(0.75DWL_0) + 0.35(0.9SL_2)$
ULC 13	$1.25DL_0 + 1.4DWL_0 + 0.5SL_2$	SLC 13	$1.0(0.75DWL_0) + 0.35(0.9SL_3)$
ULC 14	$1.25DL_0 + 1.4DWL_0 + 0.5SL_3$	SLC 14	$1.0(0.75DWL_0) + 0.35(0.9SL_4)$
ULC 15	$1.25DL_0 + 1.4DWL_0 + 0.5SL_4$	SLC 15	$1.0(0.75DWL_0) + 0.35(0.9SL_5)$
ULC 16	$1.25DL_0 + 1.4DWL_0 + 0.5SL_5$	SLC 16	$1.0(0.75UWL_0)$
ULC 17	$0.9DL_0 + 1.4UWL_0$	SLC 17	$1.0(0.75UWL_1)$
ULC 18	$0.9DL_0 + 1.4UWL_1$	SLC 18	$1.0(0.75UWL_2)$
ULC 19	$0.9DL_0 + 1.4UWL_2$	SLC 19	$1.0(0.75UWL_3)$
ULC 20	$0.9DL_0 + 1.4UWL_3$	SLC 20	$1.0(0.75UWL_4)$
ULC 21	$0.9DL_0 + 1.4UWL_4$	SLC 21	$1.0(0.75UWL_5)$
ULC 22	$0.9DL_0 + 1.4UWL_5$		

[a]Importance factors of 0.75 and 0.9 are applied to wind and snow loads, respectively, for SLS combinations (NRC 2020).

4.4 Section Selection and Design Checks

For design, structural steel conforming to ASTM A992 (ASTM 2022) is assumed, with F_y = 345 MPa, F_u = 450 MPa, E = 200 GPa, and G = 76.9 GPa. Rolled wide-flange sections listed in the Handbook of Steel Construction (CISC 2021) are considered in the design. For each overhanging girder and each LRC, the lightest section satisfying all applicable design checks is selected. The checks considered in the section-selection process include: (1) moment resistance, accounting for plastic hinge formation and LTB in accordance with the design method described in Section 3.2; (2) the effect of tension-flange bolt holes on moment resistance, assuming two 23.8-mm-diameter (15/16-in.) bolt holes for 22.2-mm-diameter (7/8-in.) bolts at a single cross-section, with M_p reduced as required in accordance with Section 3.3; (3) shear, including yielding and buckling, according to CSA S16-24; (4) web yielding and crippling at load-application points, including column lines; and (5) deflections under the SLS load combinations—limited to an allowable deflection Δ_a, taken as $L_b/240$ for the back span and $L_c/120$ for the cantilever—consistent with recommendations for industrial buildings with inelastic roof coverings (CSA 2024).

Table 4 presents moment ratios, moment resistances, and utilization ratios for the double-overhanging girder under LRCs 1 and 4, while Table 5 provides the corresponding results for LRCs 2, 3, and 5 (LRCs within each set produce identical bending-moment distributions for a given load combination). The tables correspond to the ULS load combinations and report results only for the lightest section selected under each LRC; the selected sections are identified in the tables. In these tables, M_f is the factored moment demand, taken as the absolute value of M_{max}. Values of $\Omega_2 \geq 1.00$ indicate that plastic hinge formation governs (i.e., $M_r = \phi M_p$), whereas

$\Omega_2 < 1.00$ indicates that LTB governs. All selected sections are classified as Class 1, except for the W530×82 section, which is classified as Class 2 due to its flange slenderness.

For the double-overhanging girder under LRC 1, detailed flexural-design calculations are presented for one representative load combination—ULC 7—out of the 22 considered. The selected load combination, ULC 7, is not the governing case (i.e., the one with the highest utilization ratio); instead, it is chosen to demonstrate the application of the design method for a case in which LTB, rather than plastic hinge formation, governs. Fig. 7 presents the bending-moment diagram (BMD) and required moment components for the girder under ULC 7. Table 6 provides the corresponding detailed flexural-design calculations. In this table, d_h is the bolt-hole diameter, and $M_{p,r}$ denotes the reduced M_p calculated using Z_e, as defined in Section 3.3.

4.5 Discussion of Results

Table 7 summarizes the critical utilization ratios for flexure, shear, bearing, and service-level deflection, along with the governing load combinations, for both single- and double-overhanging girders under all five LRCs. In this table, V_f and B_f denote factored shear and bearing demands, respectively; V_r and B_r are the corresponding factored resistances in accordance with CSA S16-24; and Δ is the vertical deflection under service-level loading. Key observations are as follows:

- Shear and bearing utilization ratios are consistently well below 1.00, indicating that these limit states are significantly less critical than flexure or vertical deflection. Among the 10 design cases considered—covering two girder types (single- and double-overhanging) and five LRCs—eight are governed by flexure and two by serviceability (vertical deflection).
- All bearing utilization ratios are less than 1.00. Consequently, web stiffeners are not required at load-application points; however, at column lines, pairs of web stiffeners with a thickness of 9.5 mm (3/8 in.) are provided. The resulting stiffener width-to-thickness ratios for the W530×82, W610×82, W610×92, W610×101, and W460×106 sections are 8.9, 7.3, 7.3, 10.0, and 7.9, respectively—all of which are less than the local buckling limit (i.e., $200/(F_{ys})^{0.5} = 10.8$, given $F_{ys} = 345$ MPa).
- Vertical deflection at the cantilever tip is more critical than in the back span, particularly under SLC 2, which combines the partial-pattern live load LL_1 (i.e., L_F applied only in the back-span bays) with the full-pattern downward wind load DWL_0, using the prescribed load factors.
- Upward wind load does not govern the design in the examples considered. However, flexural utilization ratios associated with load combinations that include upward wind load (i.e., ULCs 17 through 22) reach values as high as 0.69, 0.51, 0.73, 0.47, and 0.59 for LRCs 1 through 5, respectively.
- LRC 2 consistently requires heavier girder sections due to its conservative assumption that downward cantilever loads act at the top-flange level and upward loads at the shear-center level (see Section 3.2), whereas in practice the cantilever load is shared between these two locations. Previous numerical investigations have shown that, in some cases, this assumption can substantially underestimate the moment resistance—by up to 54% when only 25% of the cantilever load is actually applied at the top flange—particularly when the negative moment at the interior support equals or exceeds the maximum positive moment in the back span (Esmaeili 2025).

Table 4: Moment ratios, moment resistances, and utilization ratios for the double-overhanging girder under LRCs 1 and 4

Load combination	M_{max} (kN·m)	M_{CL} (kN·m)	$M_{F,min}$ (kN·m)	$M_{F,max}$ (kN·m)	κ'_1	κ'_2	κ'_3	LRC 1 (W530×82)		LRC 4 (W610×82)	
								Ω_2	$\frac{M_f}{M_r}$	Ω_2	$\frac{M_f}{M_r}$
ULC 1	208	208	−162	−162	1.00	−0.78	−0.78	0.80	0.42	0.97	0.33
ULC 2	365	365	−284	−284	1.00	−0.78	−0.78	0.80	0.74	0.97	0.57
ULC 3	481	481	−168	−168	1.00	−0.35	−0.35	1.18	0.78	0.97	0.75
ULC 4	−284	101	−284	−284	−0.35	1.00	1.00	0.54	0.85	0.98	0.44
ULC 5	434	434	−337	−337	1.00	−0.78	−0.78	0.80	**0.88**	0.97	0.68
ULC 6	325	325	−253	−253	1.00	−0.78	−0.78	0.80	0.66	0.97	0.51
ULC 7	−337	283	−337	−253	−0.84	1.00	0.75	0.67	0.81	0.98	0.52
ULC 8	518	518	−253	−253	1.00	−0.49	−0.49	1.04	0.84	0.97	**0.81**
ULC 9	−337	283	−337	−253	−0.84	1.00	0.75	0.67	0.81	0.98	0.52
ULC 10	325	325	−253	−253	1.00	−0.78	−0.78	0.80	0.66	0.97	0.51
ULC 11	365	365	−284	−284	1.00	−0.78	−0.78	0.80	0.74	0.97	0.57
ULC 12	328	328	−255	−255	1.00	−0.78	−0.78	0.80	0.66	0.97	0.51
ULC 13	316	314	−284	−255	0.99	−0.90	−0.81	0.74	0.69	0.97	0.50
ULC 14	393	393	−255	−255	1.00	−0.65	−0.65	0.89	0.71	0.97	0.61
ULC 15	316	314	−284	−255	0.99	−0.90	−0.81	0.74	0.69	0.97	0.50
ULC 16	328	328	−255	−255	1.00	−0.78	−0.78	0.80	0.66	0.97	0.51
ULC 17	−50	−50	39	39	1.00	−0.78	−0.78	0.44	0.19	0.51	0.15
ULC 18	51	51	−40	−40	1.00	−0.78	−0.78	0.80	0.10	0.97	0.08
ULC 19	96	91	−40	39	0.94	−0.41	0.41	1.43	0.16	0.97	0.15
ULC 20	−129	−129	−40	−40	1.00	0.31	0.31	0.31	0.68	0.46	0.43
ULC 21	96	91	−40	39	0.94	−0.41	0.41	1.43	0.16	0.97	0.15
ULC 22	51	51	−40	−40	1.00	−0.78	−0.78	0.80	0.10	0.97	0.08

Note: The critical utilization ratio under each LRC is shown in boldface.

Table 5: Moment ratios, moment resistances, and utilization ratios for the double-overhanging girder under LRCs 2, 3, and 5

Load combination	M_{max} (kN·m)	M_{CL} (kN·m)	$M_{F,min}$ (kN·m)	$M_{F,max}$ (kN·m)	κ'_1	κ'_2	κ'_3	LRC 2 (W460×106)		LRC 3 (W610×82)		LRC 5 (W610×82)	
								Ω_2	$\frac{M_f}{M_r}$	Ω_2	$\frac{M_f}{M_r}$	Ω_2	$\frac{M_f}{M_r}$
ULC 1	−206	165	−206	−206	−0.80	1.00	1.00	0.65	0.43	0.74	0.42	0.98	0.32
ULC 2	−361	289	−361	−361	−0.80	1.00	1.00	0.65	0.75	0.74	0.74	0.98	0.56
ULC 3	435	435	−214	−214	1.00	−0.49	−0.49	1.20	0.59	0.97	0.68	0.98	0.67
ULC 4	−361	24	−361	−361	−0.07	1.00	1.00	0.59	0.82	0.67	0.81	0.98	0.56
ULC 5	−428	343	−428	−428	−0.80	1.00	1.00	0.65	**0.89**	0.74	**0.87**	0.98	0.66
ULC 6	−321	257	−321	−321	−0.80	1.00	1.00	0.65	0.67	0.74	0.65	0.98	0.50
ULC 7	−428	203	−428	−321	−0.47	1.00	0.75	0.66	0.87	0.76	0.85	0.98	0.66
ULC 8	450	450	−321	−321	1.00	−0.71	−0.71	0.87	0.70	0.97	0.70	0.98	**0.70**
ULC 9	−428	203	−428	−321	−0.47	1.00	0.75	0.66	0.87	0.76	0.85	0.98	0.66
ULC 10	−321	257	−321	−321	−0.80	1.00	1.00	0.65	0.67	0.74	0.65	0.98	0.50
ULC 11	−360	288	−360	−360	−0.80	1.00	1.00	0.65	0.75	0.74	0.73	0.98	0.56
ULC 12	−324	260	−324	−324	−0.80	1.00	1.00	0.65	0.68	0.74	0.66	0.98	0.50
ULC 13	−360	242	−360	−324	−0.67	1.00	0.90	0.65	0.74	0.75	0.73	0.98	0.56
ULC 14	−324	324	−324	−324	−1.00	1.00	1.00	0.66	0.66	0.76	0.65	0.98	0.50
ULC 15	−360	242	−360	−324	−0.67	1.00	0.90	0.65	0.74	0.75	0.73	0.98	0.56
ULC 16	−324	260	−324	−324	−0.80	1.00	1.00	0.65	0.68	0.74	0.66	0.98	0.50
ULC 17	50	−40	50	50	−0.80	1.00	1.00	0.86	0.08	0.63	0.12	0.71	0.11
ULC 18	−51	41	−51	−51	−0.80	1.00	1.00	0.65	0.11	0.74	0.10	0.98	0.08
ULC 19	98	91	−51	50	0.93	−0.52	0.51	1.51	0.13	0.97	0.15	0.98	0.15
ULC 20	−140	−140	−51	−51	1.00	0.36	0.36	0.45	0.42	0.34	0.63	0.47	0.46
ULC 21	98	91	−51	50	0.93	−0.52	0.51	1.51	0.13	0.97	0.15	0.98	0.15
ULC 22	−51	41	−51	−51	−0.80	1.00	1.00	0.65	0.11	0.74	0.10	0.98	0.08

Note: The critical utilization ratio under each LRC is shown in boldface.

Table 6: Summary of flexural-design calculations for the W530×82 double-overhanging girder under LRC 1 and ULC 7, with d_h = 23.8 mm

Parameter/Formula	Value/Calculation	Note
Load in back span	$(1.25\times1.50+1.5\times1.46/2+0.4\times0.77)\times10\times(12/7) = 56.2$ kN	Downward
Load at left cantilever tip	$(1.25\times1.50+1.5\times1.46+0.4\times0.77)\times10\times(12/7)\times3 = 224.8$ kN	Downward
Load at right cantilever tip	$(1.25\times1.50+1.5\times1.46/2+0.4\times0.77)\times10\times(12/7)\times3 = 168.5$ kN	Downward
$b/(2t)$	$145/(345)^{0.5} = 7.81 < 209/(2\times13.3) = 7.86 < 170/(345)^{0.5} = 9.15$	Class 2 flange (CSA 2024)
h/w	$(528-2\times13.3)/9.5 = 52.8 < 1100/(345)^{0.5} = 59.2$	Class 1 web (CSA 2024)
$\rho_h = 2d_h/b$	$2\times23.8/209 = 0.23 > 0.15$	M_p reduction required
Z_n	1886×10^3 mm^3	Eq. 5
Z_e	$\min(0.05\times(2060\times10^3)+(1886\times10^3)\ ,\ 2060\times10^3) = 1989\times10^3$ mm^3	Eq. 4
$M_{p,r} = Z_eF_y$	$[(1989\times10^3)\times345]/10^6 = 686$ kN·m	Reduced M_p
EI_yGJ	$(200\times10^3)\times(20.3\times10^6)\times(76.9\times10^3)\times(518\times10^3) = 1617.8\times10^{20}$ (N·mm^2)^2	—
$(\pi E/L_b)^2I_yC_w$	$[\pi\times(200\times10^3)/(12\times10^3)]^2\times(20.3\times10^6)\times(1340\times10^9) = 745.8\times10^{20}$ (N·mm^2)^2	—
$M'_{u,b} = (\pi/L_b)[EI_yGJ+(\pi E/L_b)^2I_yC_w]^{0.5}$	$[\pi/(12\times10^3)]\times[(1617.8\times10^{20})+(745.8\times10^{20})]^{0.5}/10^6 = 127$ kN·m	Eq. 3
$\kappa'_1 = M_{CL}/M_{max}$	$283/(-337) = -0.84$	
$\kappa'_2 = M_{F,min}/M_{max}$	$(-337)/(-337) = 1.00$	Fig. 7
$\kappa'_3 = M_{F,max}/M_{max}$	$(-253)/(-337) = 0.75$	
n_c	2	Double-overhanging
ξ, ψ_0, ψ_1, ψ_2, ψ_3, ψ_4, and ψ_5	14.67, 0.51, 0.59, 0, 0.45, −0.56, and −0.04	Table 1 ($M_{max} < 0$ and $\kappa'_1 < 0$)
$M'_{u,b}/M_{p,r}$	$127/686 = 0.19$	—
$1-\kappa'_1/2$	$1-(-0.84/2) = 1.42$	—
$1-\kappa'_2/2$	$1-(1.00/2) = 0.50$	—
$1-\kappa'_3/2$	$1-(0.75/2) = 0.63$	—
Ω_2	$14.67\times(0.19)^{0.51}\times(1.42)^{0.59}\times(0.50)^{0}\times(0.63)^{0.45}\times(52.8)^{-0.56}\times(1)^{-0.04} = 0.67$	Eq. 2
$M_r = \phi\Omega_2M_{p,r} \le \phi M_{p,r}$	$0.9\times0.67\times686 = 414$ kN·m $< 0.9\times686 = 618$ kN·m	Eq. 1
M_f/M_r	$337/414 = 0.81$	—

Table 7: Critical utilization ratios and governing load combinations for single- and double-overhanging girders under all five LRCs, with d_h = 23.8 mm

Girder type	LRC	Section	Limit state[a]							
			Flexure					Shear[b]	Web yielding and crippling[c]	Vertical Deflection[d]
			Flange class (CSA 2024)	ρ_h	$\frac{M_{p,r}}{M_p}$	$\frac{M_f}{M_r}$	Governing load combination	$\frac{V_f}{V_r}$	$\frac{B_f}{B_r}$	$\frac{\Delta}{\Delta_a}$
Single-overhanging	1	W610×92	1	0.27	0.96	**0.88**	ULC 6	0.19	0.54	0.71
	2	W610×101	1	0.21	1.00	**0.99**	ULC 7	0.20	0.57	0.59
	3	W610×82	1	0.27	0.96	**0.99**	ULC 6	0.22	0.63	0.80
	4	W610×92	1	0.27	0.96	**0.91**	ULC 6	0.19	0.54	0.71
	5	W610×82	1	0.27	0.96	**0.98**	ULC 6	0.22	0.63	0.80
Double-overhanging	1	W530×82	2	0.23	0.97	0.88	ULC 5	0.22	0.60	**0.93**
	2	W460×106	1	0.25	1.00	**0.89**	ULC 5	0.19	0.37	0.88
	3	W610×82	1	0.27	0.96	**0.87**	ULC 5	0.19	0.58	0.77
	4	W610×82	1	0.27	0.96	**0.81**	ULC 8	0.19	0.58	0.79
	5	W610×82	1	0.27	0.96	0.70	ULC 8	0.19	0.58	**0.77**

[a]The critical ratio associated with the governing limit state under each LRC is shown in boldface.

[b]Critical at column lines under ULC 5 in all cases.

[c]Critical at column lines under ULC 5 for double-overhanging girders and under ULC 6 for single-overhanging girders; the bearing length, *N*, is assumed to be 200 mm. At column lines, pairs of web stiffeners with a thickness of 9.5 mm (3/8 in.) are required.

[d]Critical at the cantilever tip under SLC 2 in all cases.

5. Summary and Conclusions

This paper introduces a unified design method for predicting the moment resistance of overhanging steel girders—including the effect of tension-flange bolt holes—and demonstrates its application through representative design examples of Gerber roof-framing systems. The method is applied to both single- and double-overhanging girders in a five-bay roof-framing system for a single-story industrial building, considering five loading and restraint conditions (LRCs). The influence of pattern loading is also examined. The design process includes evaluation of flexural and shear capacities, service-level deflection, and web yielding and crippling at load-application points, including column lines. The lightest wide-flange sections satisfying both strength and serviceability requirements are selected, with explicit consideration of tension-flange bolt holes. Based on the design examples, the following conclusions are drawn:

- The proposed design method provides a consistent and practical framework for routine design of overhanging girders, eliminating the need for fragmented and potentially incompatible evaluations of the cantilever and back-span segments. Moment resistance is evaluated directly, including the effects of tension-flange bolt holes. Although originally developed within the framework of CSA S16-24, the method can also be implemented within similarly-structured provisions for flexural design, such as those in AISC 360-22.
- Shear and bearing demands are consistently noncritical in the examples considered. Of the 10 design cases examined, eight are governed by flexure and two by service-level deflection, with cantilever-tip deflection generally being more critical than back-span deflection.
- Although uplift does not govern section selection in the examples considered, load combinations including upward wind produce appreciable flexural utilization ratios (up to 0.73) and should be explicitly checked in design.
- LRC 2 consistently requires heavier girder sections due to its conservative assumption that downward cantilever loads act at the top-flange level and upward loads at the shear-center level. Previous numerical investigations indicate that, in some cases, this assumption can substantially underestimate moment resistance, with underestimation reaching up to 54% when only a portion of the cantilever load is actually applied at the top flange—particularly for bending-moment distributions dominated by negative moments at the column line.

Future research directions are as follows:

- An additional LRC should be introduced to supplement LRC 2 by allowing only a portion of the cantilever load to act at the top-flange level, with the remainder applied at the shear-center level. The existing LRC 2 formulation would be retained as a conservative lower-bound case, while the additional condition would reduce unnecessary conservatism.
- While the proposed design method assumes effective restraint against both lateral displacement and cross-sectional twisting at column lines, practical design guidance for bottom-flange bracing remains limited. Predictive expressions for the required stiffness and strength of bottom-flange bracing systems are therefore needed to support consistent and reliable application of the method.

Acknowledgments

This research was supported by the Natural Sciences and Engineering Research Council (NSERC) of Canada and the Canadian Institute of Steel Construction (CISC). The authors also acknowledge the support of the CISC Centre for Steel Structures Education and Research (the Steel Centre) at the University of Alberta. The contributions and technical insights provided by the industry advisory group—Charles Albert, Logan Callele, Elie Chakieh, Hesham Essa, Michael Holleran, Mark Lasby, Ian MacPhedran, Andy Metten, Ranka Radonjic-Vuksanovic, Samuel Richard, Elie Saint-Onge, Michael Samuels, Andrew Voth, Ichiro Watanabe, and Alfred Wong—are gratefully acknowledged. The first author further acknowledges financial support from the Government of Alberta through the Alberta Graduate Excellence Scholarship; from CISC through the G.L. Kulak Scholarship for Steel Structures Research; from the Structural Stability Research Council (SSRC) through the Vinnakota Award; and from the CWB Welding Foundation and the Steel Centre through the CWB Foundation Welding Advancement Award.

References

American Institute of Steel Construction (AISC). 2022. *Specification for structural steel buildings*. ANSI/AISC 360-22. Chicago, IL: AISC.

American Society for Testing and Materials (ASTM). 2022. *Standard specification for structural steel shapes*. ASTM A992/A992M-22. West Conshohocken, PA: ASTM.

Canadian Institute of Steel Construction (CISC). 1989. *Roof framing with cantilever (Gerber) girders and open-web joists*. Markham, ON: CISC.

Canadian Institute of Steel Construction (CISC). 2019. *Design module 3: Gerber roof girders*. Markham, ON: CISC.

Canadian Institute of Steel Construction (CISC). 2021. *Handbook of steel construction*. 12th ed. Markham, ON: CISC.

Canadian Standards Association (CSA). 2024. *Design and construction of steel structures*. CSA S16-24. Toronto, ON: CSA.

Datoo, Z. 2025. *Stability response of double-overhanging steel girders*. MSc thesis, Department of Civil and Environmental Engineering, University of Alberta, Edmonton, AB. https://doi.org/10.7939/83537.

Esmaeili, V. 2025. *Stability response and design of overhanging steel girders*. PhD dissertation, Department of Civil and Environmental Engineering, University of Alberta, Edmonton, AB. https://doi.org/10.7939/83309.

Esmaeili, V., A. Imanpour, and R. G. Driver. 2025. "Critical evaluation of design methods for overhanging steel girders." *Journal of Structural Engineering*, 151 (9): 04025136. https://doi.org/10.1061/JSENDH.STENG-14274.

Essa, H. S., and D. J. L. Kennedy. 1994. "Design of cantilever steel beams: refined approach." *Journal of Structural Engineering*, 120 (9): 2623–2636. https://doi.org/10.1061/(ASCE)0733-9445(1994)120:9(2623).

Essa, H. S., and D. J. L. Kennedy. 1995. "Design of steel beams in cantilever–suspended-span construction." *Journal of Structural Engineering*, 121 (11): 1667–1673. https://doi.org/10.1061/(ASCE)0733-9445(1995)121:11(1667).

Essa, M. 2024. *Full-scale tests on stability of cantilevered steel girders*. MSc thesis, Department of Civil and Environmental Engineering, University of Alberta, Edmonton, AB. https://doi.org/10.7939/r3-y89c-4n72.

Essa, M., R. G. Driver, and A. Imanpour. 2024. "Experimental testing of single-overhanging I-shaped steel girders." In *Proceedings of the Annual Stability Conference*. San Antonio, TX: Structural Stability Research Council.

Galambos, T. V. 1988. *Guide to stability design criteria for metal structures*. 4th ed. New York: John Wiley & Sons.

Imanpour, A. 2024. "Design guidelines for enhanced stability of steel systems." In *Proceedings of the Annual Stability Conference*. San Antonio, TX: Structural Stability Research Council.

Kirby, P. A., and D. A. Nethercot. 1979. *Design for structural stability*. London: Granada Publishing.

National Research Council (NRC) of Canada. 2020. *National building code of Canada*. Ottawa, ON: NRC.

Nethercot, D. A. 1973. "The effective lengths of cantilevers as governed by lateral buckling." *The Structural Engineer*, 51 (5): 161–168.

Trahair, N. S. 1983. *Lateral buckling of overhanging beams*. London: Granada Publishing.

Yura, J. A., and T. A. Helwig. 2010. "Buckling of beams with inflection points." In *Proceedings of the Annual Stability Conference*, 761–780. Orlando, FL: Structural Stability Research Council.